Journal of Ultrafine Grained and Nanostructured Materials
https://jufgnsm.ut.ac.ir
Vol. 50, No.1, June 2017, pp. 6-15
Print ISSN: 2423-6845 Online ISSN: 2423-6837
DOI: 10.7508/jufgnsm.2017.01.02

Mechanical Behavior of an Ultrafine/Nano Grained Magnesium Alloy

Seyed Mahmood Fatemi*[*,1], Abbas Zarei-Hanzaki[2]

[1]*School of Mechanical Engineering, Shahid Rajaee Teacher Training University, 136-16785, Tehran, Iran.*
[2]*Department of Metallurgical & Materials Engineering, University of Tehran, 515-14395, Tehran, Iran.*

Recieved: 20 May 2017; Accepted: 6 June 2017
** Corresponding author email: mfatemi@ut.ac.ir*

ABSTRACT

The application of magnesium alloys is greatly limited because of their relatively low strength and ductility. An effective way to improve the mechanical properties of magnesium alloy is to refine the grains. As the race for better materials performance is never ending, attempts to develop viable techniques for microstructure refinement continue. Further refining of grain size requires, however, application of extreme value of plastic deformation on material. In this work, an AZ31 wrought magnesium alloy was processed by employing multipass accumulative back extrusion process. The obtained microstructure, texture, and room temperature compressive properties were characterized and discussed. The results indicated that grains of 80 nm to 1 μm size were formed during accumulative back extrusion, where the mean grain size of the experimental material was reduced by applying successive ABE passes. The fraction of DRX increased and the mean grain size of the ABEed alloy markedly lowered, as subsequent passes were applied. This helped to explain the higher yield stress govern the occurrence of twinning during compressive loading. Compressive yield and maximum compressive strengths were measured to increase by applying successive extrusion passes, while the strain-to-fracture dropped. The evolution of mechanical properties was explained relying on the grain refinement effect as well as texture change.

Keywords: *Magnesium; Nano Grain; Twinning; Compression.*

How to cite this article:
Fatemi SM, Zarei-Hanzaki A. Mechanical Behavior of an Ultrafine/Nano Grained Magnesium Alloy. J Ultrafine Grained Nanostruct Mater, 2017; 50(1):6-15.
DOI: 10.7508/jufgnsm.2017.01.02

1. Introduction

Nanostructured and ultrafine grained materials represent the subject of numerous studies motivated by their outstanding mechanical properties and high technological potentials [1, 2]. The thrust behind the processing of bulk materials has led to the development of severe plastic deformation (SPD) in order to process the fine-grained materials. SPD has proven capability of increasing both the strength and ductility of metals as well as producing materials that exhibit high strain rate superplasticity [3, 4]. Though most SPD processing was limited to soft metals and alloys, more recent attention has focused on the processing of difficult-to-work materials such as magnesium-based alloys. Special properties such as high specific strength, damping capacity and high potential for recycling make magnesium alloys very attractive to the transportation and aerospace industries. The processing of many magnesium alloys are relatively difficult at low temperatures owing to the low symmetry hexagonal crystal structure, resulting

in the development of substantial cracking or segmentation. Also, SPD processing should be carried out at high temperatures to prevent cracking. As a result, the occurrence of dynamic recrystallization and growth occur inevitably and thereby may diminish the grain refinement effect. The post-SPD mechanical properties result from the combined effects of grain refinement and crystallographic texture changes. Furthermore, it has been demonstrated that the degree of grain refinement by SPD, itself, is strongly coupled to the development of texture and substructural evolutions [5, 6]. It has been proposed that grain refinement is primarily the result of the interaction of shear plane with texture and the crystal structure, followed by an influence coming from the accumulation of shear strain during severe deformation [5]. It has been known that moderate-to-strong level of complex textures can be induced during SPD of magnesium alloys.

Reported results on the mechanical properties of SPDed magnesium alloys illustrated that a miscellaneous combination of strength and ductility alterations may be obtained, depending on synergistic or antagonistic effects of grain refining and texture change [7, 8]. Furthermore it was recognized that the Hall–Petch parameters are texture dependent so that easy activation of basal slip introduces lower values, while inhibition of basal slip leads to higher values [9]. Kim et al. [10] reported that the yield stress of a wrought AZ61 alloy processed by eight equal channel angular pressing (ECAP) passes dropped appreciably as compared to the initial material, while the tensile ductility was significantly increased. The latter observation describes a case where the texture softening is dominant over the strengthening due to grain refinement. However, results of opposite trend were obtained by Xing et. al. [11]and Zuberova et. al. [12], where severe plastic deformation of AZ31 alloy gave rise to an increased strength accompanied by minor ductility. Dissimilarly, the results reported by Miura et. al. [13] on multi-axial forging of AZ61 alloy implied that although the tensile strength increased with a decrease in grain size, the ductility was not spoiled.

The literature is clear, on the fact that the flow stress behavior of magnesium in compression usually differs markedly from that seen in tension. For example, the contribution of twinning, strain rate sensitivity and plastic instability of Mg alloys in compression is different from that in tension [12, 14]. Very few systematic researches could be found in the literature focusing on the compressive deformation behavior of ultrafine/ nano grained magnesium alloys. The results reported by Zúberová et. al. [12] indicated that compressive yield strength of an AZ31 alloy was increased after applying four ECAP passes. On the other hand, strain-to-failure was found to drop with decreasing grain size. However, no explanation was given for the latter observation.

A continuous SPD process, so-called accumulative back extrusion process (ABE), which is appropriate for production of ultrafine/ nano grained bulk material has been introduced by present authors [15]. Previous works mainly dealt with the developed strain patterns [16], microstructure [17] and texture evolutions [18] during ABE processing. The present research was initiated to examine the compressive deformation behavior of a wrought AZ31 magnesium alloy subjected to various ABE processing. Moreover, the effect of number of passes has been evaluated through discussing combined influence of grain refinement and texture evolution.

2. Experimental procedure

A commercial AZ31 alloy (Mg-2.9Al-0.9Zn-0.7Mn, %wt), received in the form of rolled plate, was used as experimental alloy. Cylindrical samples for ABE processing were machined with the dimensions of H8×Φ18 mm2. Briefly, the first step of ABE consists of the back extrusion of the workpiece into the gap between the inner punch and the die. In the second step the back extruded material is forged back to the initial cross section by the outer punch completing one ABE cycle. The previous work showed that an average equivalent strain of 2 is induced during each step [16]. ABE process was conducted at a ram speed of 5 mm/ min and temperature of 280°C. The temperature was controlled using a K-type thermocouple which was fixed on the die wall near the inner surface. According to the relatively low stroke speed the temperature increasing during extrusion was ignored. The MoS_2 spray was used to reduce the friction between the work piece and the tool surfaces. The initial material showed a mean grain size of 25 μm (Fig. 1a). The texture of initial material was illustrated in Fig. 1b, where a strong fiber texture with most of the basal planes aligned parallel to the RD–TD plane.

For all the samples, the center of the

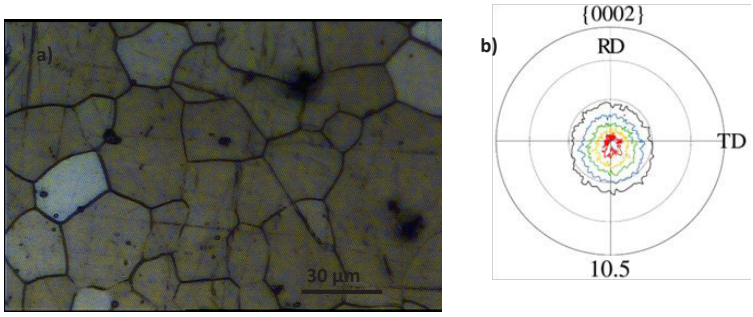

Fig. 1- a) Initial microstructure, b) measured basal pole figure of the experimental as-rolled AZ31 alloy.

rectangular cross section was considered for representative metallographic observations and x-ray measurement (as displayed in Fig. 2a). Crystallographic texture measurements were conducted using X-ray diffraction in the reflection geometry with a four circle goniometer and Cu Ka radiation. Experimental (10–10), (0002), and (10–11), pole figures were collected on a 5°× 5° grid for sample tilts, α = 0–85°, and azimuthal rotations, φ=0–355°. Background and defocusing corrections were made using experimentally determined data from random powder samples. The texture samples were sections from the flow plane (or ED–TD plane in Fig. 2b) and the texture measurements of all the samples were made parallel to the extrusion axis. The microstructures of the deformed material were examined through optical microscopy, transmission electron microscopy (TEM) and field emission scanning electron microscopy (FESEM). The SESEM study was carried out using a Zeiss Ultra Plus microscope operated at 10 kV. The TEM investigation was performed using a Philips CM 20 microscope worked at 200 kV. A slice of the ABEed work-pieces was first cut parallel to the extrusion direction. The slice was then thinned by grinding to a sheet with 100 µm thickness. The TEM samples were then mechanically polished using a twin-jet polishing unit. The perforation was done by a solution of 1% perchloric acid, 99% ethanol at a polishing temperature of 275 K.

Cylindrical samples having a diameter of 5 mm and a height of 7.5 mm were used for compression tests. Samples prepared from as-received rolled material were taken parallel to the rolling axis. Samples from the ABE processed material was machined parallel to the ABE direction (as shown in Fig. 2b). Compression tests were performed using a universal testing machine at room temperature with an initial strain rate of 10^{-4} s^{-1}. After the test, the samples were sectioned parallel to deformation direction, grinded, polished, and etched by Acetic Picral solution for further microstructural studies.

3. Results and discussion

The microstructural observations demonstrated that an outstanding grain refinement took place through ABE processing, where a relatively homogeneous grain refinement was achieved after sixth pass. TEM observation showed that recrystallized areas include grains of 90 nm to 1.5 µm. Figures 3(a), (b), and (c) typically show the microstructure of the ABE-processed AZ31 alloy up to one, two, and six passes, respectively. The ultrafine/ nano-grains developed during deformation are depicted in Figure 3(d). As the experimental alloy was processed by successive passes, the coarse grain was substituted by fine recrystallized grains and more homogenous

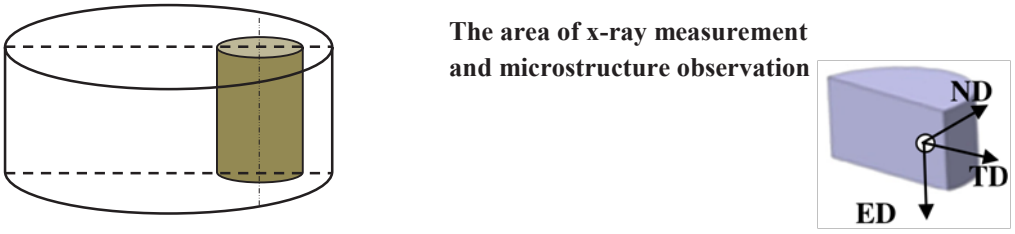

Fig. 2- Schematic illustration of the orientations of compression specimens used in deformation tests. (left) and locus of characterization (right).

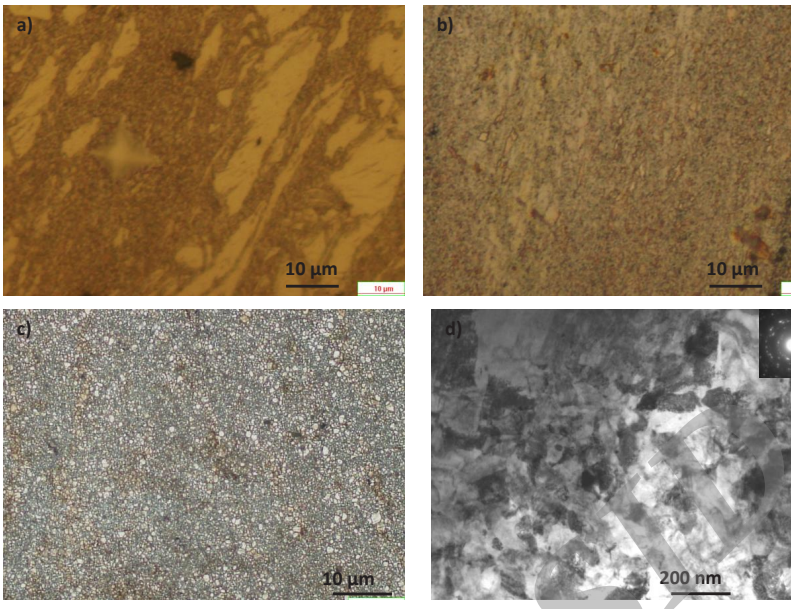

Fig. 3- Microstructure of the experimental alloy deformed up to a) one, b) two, c) four passes at 280 °C, d) ultrafine/nano grains formed after two-pass ABE processing.

microstructure was obtained. The average grain sizes were measured to be about 10, 3, and 0.5 µm after processing of one, two, and four ABE passes, respectively. As discussed in Ref. [19], discontinuous dynamic recrystallization was found as the dominant grain refinement mechanism in AZ31 experimental alloy during the early ABE pass; thereafter the dynamically recrystallized grains, in turn, were repetitively refined through continuous dynamic recrystallization upon applying successive passes. To understand the evolution of substructure and development of fine grains during successive ABE passes, EBSD maps of the material deformed up to different ABE passes were obtained from ED-TD plane. Figure 4 shows the distributions of the misorientation angles in terms of cumulative frequency (frequency of and below a given misorientation angle) of low angle boundaries (LABs) and high angle boundaries (HABs) in the samples ABEed at 280 °C. It indicates that the frequency of LABs with misorientation angles below 15° increased after single ABE, which confirms the operation of extensive dynamic recovery. However, the frequency of LABs decreases but that of HABs increases with applying successive passes. The decrease in LABs (misorientation below 15°) may indicate the transformation of LABs to HABs by incorporating the dislocations that generate during deformation. The latter requires new grain boundary area to be continuously created during deformation. This is consistent with the increase in frequency of HABs. Previous results showed that the microstructure is repetitively refined though subdivision of the dynamically recrystallized (DRXed) grains into finer ones [19].

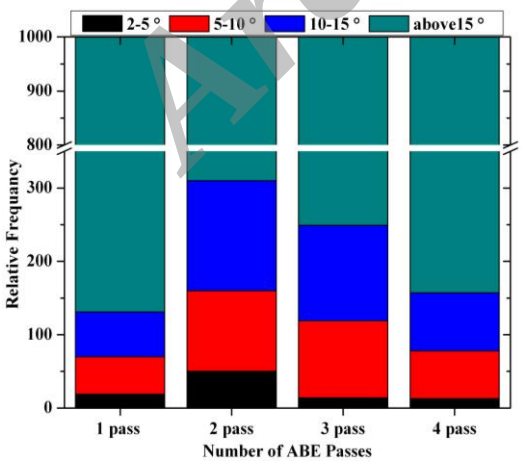

Fig. 4- The cumulative frequency of boundaries with different misorientation angle in AZ31 alloy deformed to various number of ABE passes [19].

The basal, prismatic and pyramidal pole figures of the sample deformed by different ABE passes were measured. The results were presented elsewhere [18], however, for the sake of convenience, the pole figures from the materials after the first pass are including in Fig. 5. As realized the original texture (Fig. 2b) was completely replaced and a new texture

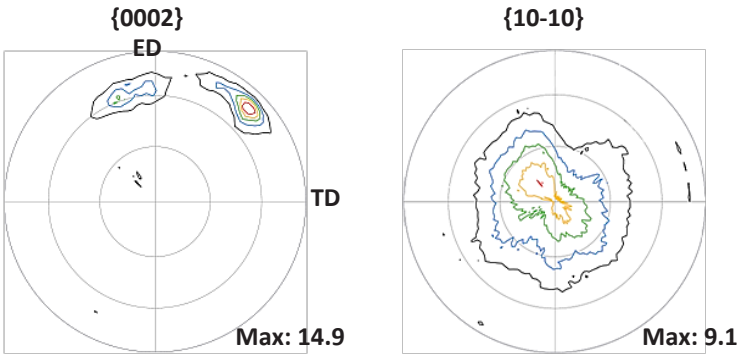

Fig. 5- (0002) and (10–10) pole figures of the texture of the experimental alloy after single ABE pass.

developed during the first pass. The obtained ABE texture corresponds to the basal poles lying ~40° away from the transverse direction (TD) in the ED–TD plane and 66° from the normal direction (ND) in the TD–ND plane, while the maximum of prismatic planes were revealed at 40–50° in the TD–ED plane. These texture components mostly place the magnesium crystal inclined to the ABE axis.

Fig. 6 depicted the compressive true stress-strain curves obtained from the as-received as well as ABEed samples. As can be seen the mechanical properties was significantly altered after deformation. The data of yield stress (YS), maximum compressive strength (MCS) and fracture strain are summarized in Fig. 6a. As simply seen, the yield stress increases almost two times after the first pass. After that it continues to be increased as subsequent passes were applied. The MCS slightly increased after the first pass, while it dropped by applying the second pass and continue to ascend again by subsequent passes. The fracture strain was decreased from 0.17 for as-received material to below 0.05 after six ABE passes. In case of pure magnesium it was reported that ECAP processing resulted in a ultrafined microstructure (d_{ave}=0.8 μm) accompanied with a enhanced both MCS and fracture strain [20]. Similar results were obtained by Ghosh and Yong [21] for an AZ31 alloy deformed by Alternate biaxial reverse corrugation. It is worth noting that the ABEed alloy exhibits serrated flow during compression which resembles that observed by Trojanova and Caceres in aged AZ91 magnesium alloy [22, 23]. They related the latter phenomenon to the strain aging of Al atoms and development of small bands to the point of suppressing the attendant homogeneous deformation. The correlation between grain size and yield stress based on Hall–Petch relation was established in Figure 7. It is obvious that the data belonging to the material processed at 230 and 280 °C preserve a same slope, while that of 180°C fits with a different slope. Accordingly, on may conclude that the deformation mechanisms for the

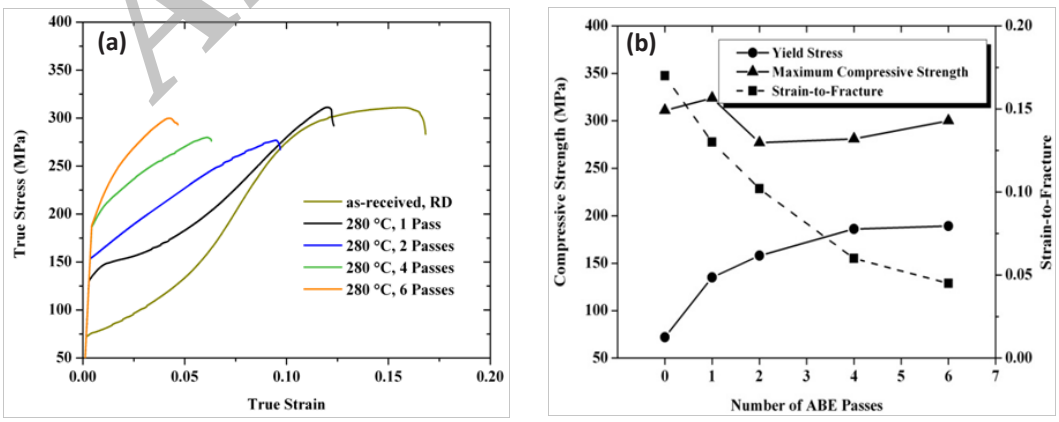

Fig. 6- a) True stress versus true strain at room temperature for as-received and processed experimental alloy, b) Variation of the yield stress, MCS and fracture strain with the number of ABE passes.

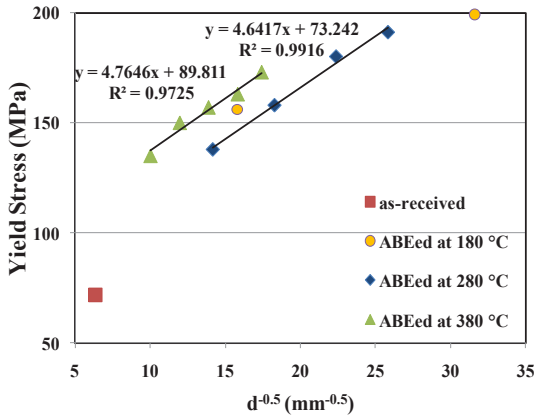

Fig. 7- The Hall–Petch correlation of compressive yield stress and grain size for the as-received material and multi-pass processed alloys.

material processed at the two higher temperatures are almost identical. The data of material processed at 180 °C fits to a different line because of the different DRX fraction and different texture. Because the data was not enough for plotting a line (just two data), the related line was not presented in the figure. The data of as-received alloy is out of line with the ones obtained from processed materials. The decreased yield strength of the as-received alloy comparing the plotted Hall–Petch correlation is related to the different deformation modes dominating at the beginning of plasticity, which will be further discussed in following paragraphs.

One way to quantify the texture data is to use the crystallite orientation distribution function (ODF), which essentially describes the frequency of the occurrence of particular orientations in a three-dimensional (Euler) orientation space. To identify the degree to which twinning and/or slip systems contribute during tensile deformation of ABEed materials, the ODFs were obtained from x-ray diffraction texture data on the basis of spherical harmonics with positivity correction according to Dahms and Bunge [24]. The ODFs are typically depicted for one and two-pass processed materials in Fig. 8. Accordingly, the crystallographic plane and direction which lie, in most of grains, parallel to the extrusion direction of ABEed samples (and thus parallel to tension axis) could be defined. The corresponding Euler angles, planes, and directions were given in Table 1. The defined directions correspond to the deformation axis of the compression samples. The Schmid factors for activating different mechanisms were calculated considering the crystallographic compression axis and the planes and directions related to each twinning and slip systems. The HCP crystal lattice of magnesium features the six equivalent twinning planes, the Schmid factors of which can be calculated numerically for any possible orientation in the textured polycrystalline alloy. For the twinning systems, the variant with maximum Schmid factor and for the slip systems the average values of Schmid factors were considered as effective Schmid factors. For the samples with two intensity peaks, the values proposed by the two were averaged out.

In the as-received material most grains have basal poles aligned with almost perpendicular

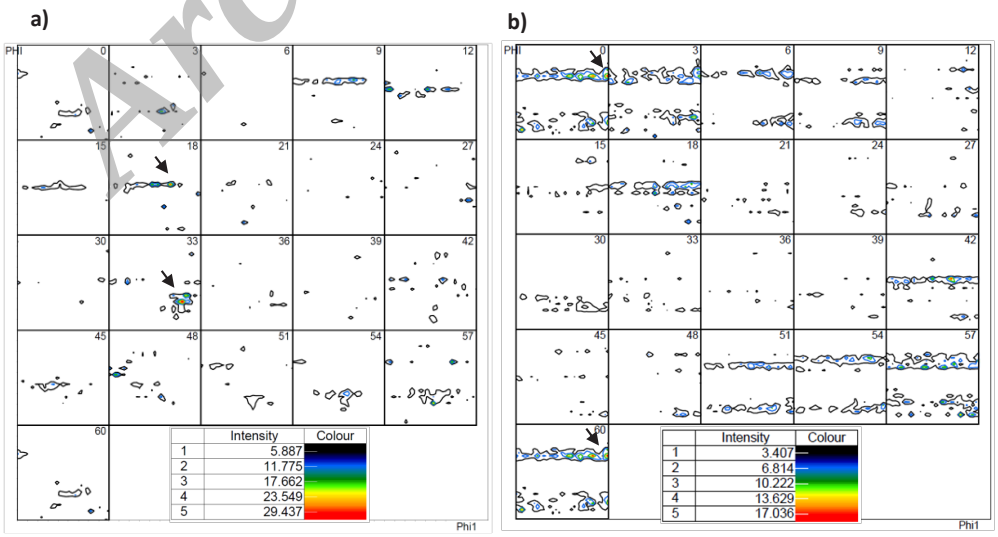

Fig. 8- ODF sections measured from the processed AZ31 alloy ABEed up to a) one pass, b) two passes.

Table 1- Absolute Schmid factors calculated for deformation mechanisms in multi-pass ABEed AZ31 alloy.

Pass Number	g{φ1,φ,φ2}	sample axis	Schmid factor									
			Tensile twinning		Basal slip		Prismatic slip		Pyramidal slip <c+a>		Pyramidal slip <a>	
			// RD	// ND	// RD	// ND	// RD	// ND	// RD	// ND	// RD	// ND
0	{81,0,57}	≅ (0001) < $1\bar{2}10$ >	0.42	0.00	0.00	0.00	0.00	0.45	0.44	0.39	0.06	0.42
1	{60,45,18}	≅ ($01\bar{1}1$) < $1\bar{2}11$ >	// ED 0.25	// TD 0.11	// ED 0.38	// TD 0.15	// ED 0.22	// TD 0.25	// ED 0.15	// TD 0.25	// ED 0.24	// TD 0.35
2	{90,30,60}	≅ ($11\bar{2}1$) < $\bar{1}\bar{1}21$ >	0.29	0.11	0.27	0.11	0.20	0.13	0.15	0.39	0.35	0.15
4	{39,45,18}	≅ ($01\bar{1}1$) < $1\bar{1}01$ >	0.41	0.02	0.27	0.08	0.15	0.24	0.32	0.4	0.26	0.37

to the RD, which favors the tensile twinning during compressive loading [25]. Therefore, the deformation during compression along the RD will be accommodated mostly by tensile twining. The strain hardening behavior observed along the RD is consistent with the activation of twins, i.e. a plateau region with relatively steady stress followed by an upward curvature with a high hardening rate. According to the Table 1, the orientation factor calculated for the activation of twinning is still high enough in single-pass processed material. However, it should be noted that due to the grain refinement introduced during ABE, the critical stress required for twinning was significantly increases. This may lead to a marked increase in yield strength. Microstructure investigation (Fig. 9) showed the prevalence of twinning in the as-received alloy, whereas the twinning was suppressed in the processed material. This caused the shape of the flow curve to change from "concave" for the as-received to "convex" for the processed samples. According to Rohatgi [26] twinning arrest the drop in strain hardening rate because it effectively decreases the grain size. Moreover, in case of magnesium, the hardening effect of twin boundaries as well as hard texture developed within the twin bands increase the strain hardening rate as the stain progressed [27]. Thus a concave-shape curve forms during the prevalence of twinning.

As subsequent passes were applied, the fraction of DRX increased and the mean grain size of the ABEed alloy markedly lowered. This may help to explain the higher yield stress govern the occurrence of twinning during compressive loading. Moreover, the latter was accompanied by a change in flow curve shape. Meyer et. al. [28]

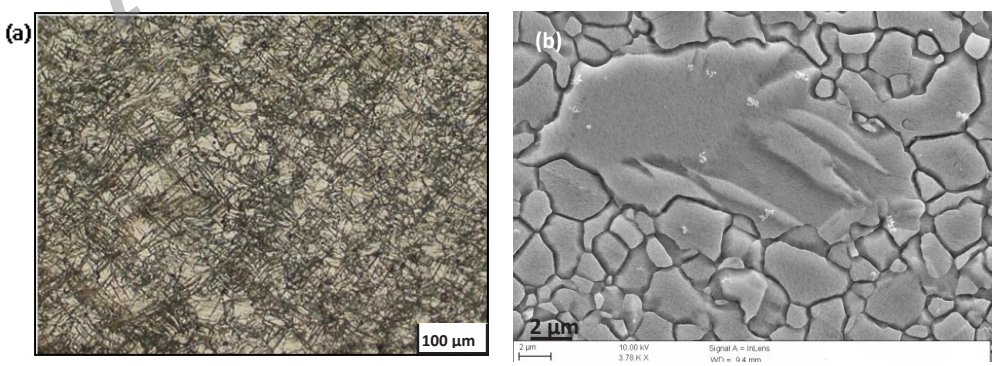

Fig. 9- The microstructure of a)as-received, b) four-pass ABEed experimental alloy deformed to 0.05 compressive strain.

pointed out that grain size dependence of twinning stress is significantly larger as compared to slip stress. Also, with increasing defamation passes, the intensity of basal texture is weakened (see Fig. 8), thus the share of easy glide on basal plane during deformation is limited. Further results on this issue was presented in Ref. [18]. Previous works has denoted that the occurrence of twinning is stopped in AZ31 alloy at a grain size of 3 μm [14, 29] and 3.4 μm [30]. However, present results shows evidence of twins at grains as fine as 1-2 μm (Fig. 9).

As twinning is suppressed, the operation of basal slip is considered as the major mechanism during compressive deformation of the processed materials. According to the reported data, the critical resolved shear stresses (CRSS) for basal slip AZ31 alloy is 2 MPa [31]. Thus it can be simply provided during compression tests of the ABEed alloy. However, lower mean grain sizes of the alloy introduce higher strengthening for basal slip-dominated flow. Moreover, since the intensity of basal plane was decreased in multi-pass ABEed alloy, the contribution of easy basal slip is expected to be reduced.

A change in deformation mechanisms with decreasing grain size may give a plausible explanation for the decrease in hardening rate. Beside suppression of twinning which means a reduction in twin induced hardening, texture hardening should be taken into account. The weakening of basal texture with increasing number of deformation passes, may give rise to the premature activation of non-basal slip during compression. The data in Table 1 implied that both prismatic and pyramidal slip favors in the ABEed materials. According to the lower CRSS for prismatic slip, compared with pyramidal slip, a higher relative activity of prismatic is anticipated. However, the CRSS for pyramidal slip is so large and Koike [32] reported that when the compressive flow stress increases to a large value of more than 200 MPa the activation of the <c+a> slip is possible. Because of constraint by neighboring grains in polycrystalline magnesium, strain incompatibility at grain boundaries may cause additional stress [33]. This compatibility stress gives rise to the activation of nonbasal dislocations in the region within several microns from grain boundaries [32]. So it is rationalize to assume that the compatibility stress influences the entire grain volume in the ultrafine/nano grained magnesium. Thus, the compatibility stress may provide the CRSS for the activation of pyramidal slip and restrict the operation of basal and prismatic slip systems. This may end up to limited workability and premature cracking in the material deformed to more passes.

FESEM results, typically showed in Fig. 10, depicted that compressive twins were developed along the boundaries. It is speculated that the high dislocation density at the vicinity of grain boundaries exhausted the local hardenability of materials, where the concentrated stress cause the development of compressive twinning. The latter features may be considered as the short cut path toward premature cracking.

4. Conclusion

Ultrafine/nano-grained microstructure was produced in AZ31 wrought magnesium alloy through multipass ABE processing. The compressive deformation behavior of an ultrafine/nano grained AZ31 magnesium alloy was evaluated by employing uniaxial compression tests. The results showed that grain refinement as well as texture modifications may increase yield and maximum compressive strain. Grain refining down

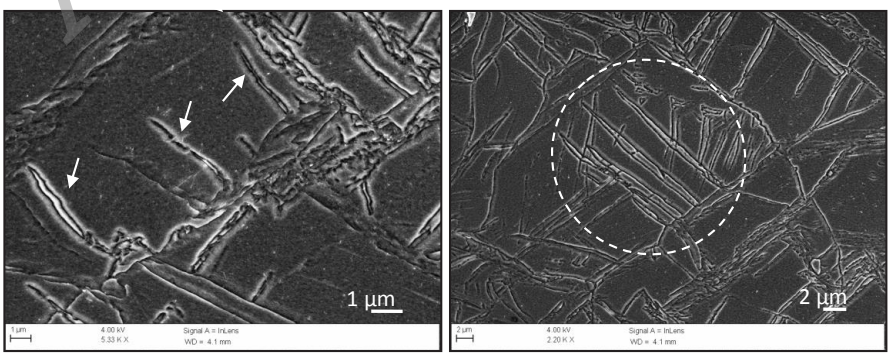

Fig. 10- The occurrence of compressive twinning at the vicinity of grain boundaries after deformation of ultrafine/nano grained AZ31 alloy.

to the ultrafine and nano scale increased the CRSS required for twinning, while the weakened intensity of basal texture concurrently invoked higher yield stress. Texture analysis implied that both prismatic and pyramidal slip possess proper orientation factor to be activated during compression test of the processed materials. The lower was the mean grain size of the experimental alloy, the higher MCS and the lower strain-to- fracture were obtained, due to the compatibility stress contribute during deformation of magnesium alloys.

References:

1. Valiev R. Nanostructuring of metals by severe plastic deformation for advanced properties. Nature Materials. 2004;3(8):511-516.
2. Khajezade A, Habibi Parsa M, Mirzadeh H, Montazeri-pour M. Grain Refinement Efficiency of Multi-Axial Incremental Forging and Shearing: A Crystal Plasticity Analysis. Journal of Ultrafine Grained and Nanostructured Materials. 2016;49(1):11-16.
3. Figueiredo RB, Langdon TG. Principles of grain refinement and superplastic flow in magnesium alloys processed by ECAP. Materials Science and Engineering: A. 2009;501(1-2):105-114.
4. Kim W, Jeong H, Jeong H. Achieving high strength and high ductility in magnesium alloys using severe plastic deformation combined with low-temperature aging. Scripta Materialia. 2009;61(11):1040-1043.
5. Wang H, Wu P, Wang J. Modelling the role of slips and twins in magnesium alloys under cyclic shear. Computational Materials Science. 2015;96:214-218.
6. Wang J, Zhang D, Li Y, Xiao Z, Fouse J, Yang X. Effect of initial orientation on the microstructure and mechanical properties of textured AZ31 Mg alloy during torsion and annealing. Materials & Design. 2015;86:526-535.
7. Biswas S, Suwas S. Evolution of sub-micron grain size and weak texture in magnesium alloy Mg–3Al–0.4 Mn by a modified multi-axial forging process. Scripta Materialia. 2012;66(2):89-92.
8. Gzyl M, Rosochowski A, Boczkal S, Olejnik L. The role of microstructure and texture in controlling mechanical properties of AZ31B magnesium alloy processed by I-ECAP. Materials Science and Engineering: A. 2015;638:20-29.
9. Yuan W, Panigrahi SK, Su JQ, Mishra RS. Influence of grain size and texture on Hall–Petch relationship for a magnesium alloy. Scripta Materialia. 2011;65(11):994-7.
10. Kim W, An C, Kim Y, Hong S. Mechanical properties and microstructures of an AZ61 Mg alloy produced by equal channel angular pressing. Scripta Materialia. 2002;47(1):39-44.
11. Xing J, Yang X, Miura H, Sakai T. Mechanical properties of magnesium alloy AZ31 after severe plastic deformation. Materials Transactions. 2008;49(1):69-75.
12. Zuberova Z, Estrin Y, Lamark T, Janecek M, Hellmig R, Krieger M. Effect of equal channel angular pressing on the deformation behaviour of magnesium alloy AZ31 under uniaxial compression. Journal of Materials Processing Technology. 2007;184(1-3):294-299.
13. Miura H, Maruoka T, Yang X, Jonas J. Microstructure and mechanical properties of multi-directionally forged Mg–Al–Zn alloy. Scripta Materialia. 2012;66(1):49-51.
14. Yang Q, Ghosh A. Deformation behavior of ultrafine-grain (UFG) AZ31B Mg alloy at room temperature. Acta Materialia. 2006;54(19):5159-5170.
15. Fatemi-Varzaneh S, Zarei-Hanzaki A. Accumulative back extrusion (ABE) processing as a novel bulk deformation method. Materials Science and Engineering: A. 2009;504(1-2):104-106.
16. Fatemi-Varzaneh S, Zarei-Hanzaki A, Naderi M, Roostaei AA. Deformation homogeneity in accumulative back extrusion processing of AZ31 magnesium alloy. Journal of Alloys and Compounds. 2010;507(1):207-214.
17. Fatemi-Varzaneh S, Zarei-Hanzaki A. Processing of AZ31 magnesium alloy by a new noble severe plastic deformation method. Materials Science and Engineering: A. 2011;528(3):1334-1339.
18. Fatemi-Varzaneh S, Zarei-Hanzaki A, Paul H. Characterization of ultrafine and nano grained magnesium alloy processed by severe plastic deformation. Materials Characterization. 2014;87:27-35.
19. Fatemi-Varzaneh S, Zarei-Hanzaki A, Cabrera J, Calvillo P. EBSD characterization of repetitive grain refinement in AZ31 magnesium alloy. Materials Chemistry and Physics. 2015;149:339-343.
20. Li J, Xu W, Wu X, Ding H, Xia K. Effects of grain size on compressive behaviour in ultrafine grained pure Mg processed by equal channel angular pressing at room temperature. Materials Science and Engineering: A. 2011;528(18):5993-8.
21. Yang Q, Ghosh A. Production of ultrafine-grain microstructure in Mg alloy by alternate biaxial reverse corrugation. Acta Materialia. 2006;54(19):5147-5158.
22. Caceres C, Davidson C, Griffiths J, Newton C. Effects of solidification rate and ageing on the microstructure and mechanical properties of AZ91 alloy. Materials Science and Engineering: A. 2002:325(1-2):344-355.
23. Trojanova Z, Caceres C. On the strain to the onset of serrated flow in a magnesium alloy. Scripta Materialia. 2007;56(9):793-796.
24. Dahms M, Bunge HJ. The iterative series-expansion method for quantitative texture analysis. I. General outline. Journal of Applied Crystallography. 1989;22(5):439-447.
25. Barnett M. Twinning and the ductility of magnesium alloys: Part II. Materials Science and Engineering: A. 2007;464(1-2):8-16.
26. Rohatgi A, Vecchio KS, Gray GT. The influence of stacking fault energy on the mechanical behavior of Cu and Cu-Al alloys: deformation twinning, work hardening, and dynamic recovery. Metallurgical and Materials Transactions A. 2001;32(1):135-145.
27. Barnett M. Influence of deformation conditions and texture on the high temperature flow stress of magnesium AZ31. Journal of Light Metals. 2001;1(3):167-177.
28. Meyers M, Vöhringer O, Lubarda V. The onset of twinning in metals: a constitutive description. Acta Materialia. 2001;49(19):4025-4039.
29. Lapovok R, Thomson P, Cottam R, Estrin Y. The effect of grain refinement by warm equal channel angular extrusion on room temperature twinning in magnesium alloy ZK60.

Journal of Materials Science. 2005;40(7):1699-1708.

30. Yin S, Wang C, Diao Y, Wu S, Li S. Influence of Grain Size and Texture on the Yield Asymmetry of Mg-3Al-1Zn Alloy. Journal of Materials Science & Technology. 2011;27(1):29-34.
31. Wang Y, Huang J. The role of twinning and untwinning in yielding behavior in hot-extruded Mg-Al-Zn alloy. Acta Materialia. 2007;55(3):897-905.
32. Koike J, Kobayashi T, Mukai T, Watanabe H, Suzuki M, Maruyama K, Higashi K. The activity of non-basal slip systems and dynamic recovery at room temperature in fine-grained AZ31B magnesium alloys. Acta Materialia. 2003;51(7):2055-2065.
33. Koike J. Enhanced deformation mechanisms by anisotropic plasticity in polycrystalline Mg alloys at room temperature. Metallurgical and Materials Transactions A. 2005;36(7):1689-1696.